HHS Public Access

Author manuscript

Biochim Biophys Acta. Author manuscript; available in PMC 2018 September 01.

Published in final edited form as:

Biochim Biophys Acta. 2017 September ; 1863(9): 2333–2341. doi:10.1016/j.bbadis.2017.06.021.

Total abdominal irradiation exposure impairs cognitive function involving miR-34a-5p/BDNF axis

Ming Cui[1,*], **Huiwen Xiao**[1], **Yuan Li**[1], **Jiali Dong**[1], **Dan Luo**[1], **Hang Li**[1], **Guoxing Feng**[1], **Haichao Wang**[1,2], and **Saijun Fan**[1,*]

[1]Tianjin Key Laboratory of Radiation Medicine and Molecular Nuclear Medicine, Institute of Radiation Medicine, Chinese Academy of Medical Sciences and Peking Union Medical College, 238 Baidi Road, Tianjin 300192, China

[2]Department of Emergency Medicine, North Shore University Hospital, Laboratory of Emergency Medicine, the Feinstein Institute for Medical Research, 350 Community Drive, Manhasset, NY 11030 USA

Abstract

Radiotherapy is often employed to treat abdominal and pelvic malignancies, but is frequently accompanied by diverse acute and chronic local injuries. It was previously unknown whether abdominal and pelvic radiotherapy impairs distant cognitive dysfunction. In the present study, we demonstrated that total abdominal irradiation (TAI) exposure caused cognitive deficits in mouse models. Mechanically, microarray assay analysis revealed that TAI elevated the expression level of miR-34a-5p in small intestine tissues and peripheral blood (PD), which targeted the 3′UTR of Brain-derived neurotrophic factor (*Bdnf*) mRNA in hippocampus to mediate cognitive dysfunction. Tail intravenous injection of miR-34a-5p antagomir immediately after TAI exposure rescued TAI-mediated cognitive impairment *via* blocking the up-regulation of miR-34a-5p in PD, resulting in restoring the *Bdnf* expression in the hippocampus. More importantly, high throughput sequencing validated that the gut bacterial composition of mice was shifted after TAI exposure, which was retained by miR-34a-5p antagomir injection. Thus, 27(7):916-932our findings provide new insights into pathogenic mechanism underlying abdominal and pelvic radiotherapy-mediated distant cognitive impairment.

Keywords

Radiotherapy; Cognitive dysfunction; Bdnf; MicroRNA; Gut microbiota

Correspondence should be addressed to Saijun Fan (fansaijun@irm-cams.ac.cn) and Ming Cui (cuiming0403@bjmu.edu.cn).

Author Contributions: study concept and design: Ming Cui and Saijun Fan; **acquisition of data:** Ming Cui, Huiwen Xiao, Dan Luo, Yuan Li, and jiali Dong; **analysis and interpretation of data:** Ming Cui and Huiwen Xiao; **drafting of the manuscript:** Ming Cui, Huiwen Xiao and Saijun Fan; **critical revision of the manuscript for important intellectual content:** Ming Cui, Haichao Wang and Saijun Fan; **statistical analysis:** Ming Cui and Huiwen Xiao; **obtained funding:** Ming Cui, Haichao Wang and Saijun Fan; **administrative, technical, or material support:** Ming Cui and Saijun Fan; **study supervision:** Saijun Fan.

Competing financial interests: The authors declare no competing financial interests

1. Introduction

Despite considerable advances in understanding the molecular basis of abdominal and pelvic neoplasms, abdominal and pelvic cancers, such as colorectal cancer, prostate cancer and cervical cancer, remain the most common form of cancer leading tumor-related mortality globally [1]; [2]; [3]. Radiotherapy is a cornerstone of modern management of malignancies and, > 50% of patients with cancer receive this treatment at some point in the course of their disease [4]. Thus far, all available cancer therapies can carry various side effects and lose effectiveness [5]. With the on-going increase in the number of cancer survivors, the prevention of radiotherapy-associated adverse effects has increasingly become a priority [6] ; [7]. Overall, the gastrointestinal (GI) syndrome is the main toxicity related to abdominal radiotherapy of human cancers [8]. Radiation exposure causes intestinal crypt damage, small intestine failure, and eventually death. However, it was previously unknown whether abdominal and pelvic radiotherapy also perturbed the function of other distal organs.

Brain-derived neurotrophic factor (BDNF), a member of a small family of secreted proteins within the hippocampus, governs multiple biological functions ranging from neuronal survival and differentiation during development to synaptic and cognitive behavior [9]. BDNF has been implicated in the modulation of energy balance [10], as alterations in its expression levels and activities result in a number of neurodegenerative disorders, covering Huntington disease, Alzheimer disease and Parkinson disease [11] ; [12]. Heretofore, it was not yet identified whether abdominal radiotherapy influenced BDNF expression in the brain. MicroRNAs (miRNAs) are small, non-coding RNAs which emerge as key post-transcriptional modulators of gene expression [13]. Previous studies reported that miR-34a-5p was implicated in development of cognitive function [14] ; [15]. The brain and gut show reciprocal interactions in health and disease, altered brain outputs have been shown to influence intestinal motility and secretion, several observed peripheral findings can feed back to the brain, setting up circular regulatory loops [16]. As an important player in this dialogue, the composition and behavior of gut microbiota might shape mental health and even neurological development [17]. Investigations in germ-free animals and animals exposed to pathogenic bacterial infections, probiotic bacteria or antibiotic drugs disclose a role for the gut microbiota and its metabolites in the modulation of anxiety, mood, cognition and pain *via* gut-brain neural circuits [18] ; [19]. However, whether abdominal radiotherapy affects cognitive function hijacking gut microbiota remains mysterious.

In this study, we employed Morris water maze test to determine whether total abdominal irradiation (TAI) impaired cognitive function in mouse models. Furthermore, we elucidated the pathogenic mechanisms underlying TAI-mediated cognitive dysfunction by characterizing the expression level of miR-34a-5p in the periphery and *Bdnf* expression in the hippocampus. To understand the pathogenic roles of miR-34a-5p and *Bdnf* in TAI-mediated cognitive impairment, miR-34a-5p antagomir was employed to assess its impact on central *Bdnf* expression and cognitive function. Finally, high throughput sequencing reveled that miR-34a-5p antagomir injection retained TAI-shifted gut microbiota. Thus, our findings provide new insights into the pathogenic mechanism underlying abdominal

radiotherapy-induced distant cognitive impairment, and shed light on the development of future therapies to attenuate radiation-mediated brain dysfunction.

2. Materials and methods

2.1. Animals

Six- to 8-week-old female C57BL/6J mice were purchased from Vital River (Beijing, China), mice were housed in the Specific Pathogen Free level animal facility at the Institute of Radiation Medicine (IRM), the Chinese Academy of Medical Sciences (CAMS). Mice were kept under standard conditions (ambient temperature 22 ± 2 °C, air humidity 40–70% and a 12/12-h light/dark cycle) and continuous access to a standard diet and water. All mice in this study were of a pure C57BL/6 genetic background and separated into groups randomly, treated according to the guidelines established by the National Institutes of Health Guide (NIH) for use. All experiments were done in accordance with procedures approved by the Daegu-Gyeongbuk Medical Innovation Foundation (DGMIF) Institutional Animal Care and Use Committee (IACUC). All procedures and animals handlings were performed following the ethical guidelines for animal studies.

2.2. Irradiation study

A Gammacell® 40 Exactor (Best Theratronics Ltd., Canada) was used for all experiments [20]. In this study, female (about 20 g in body weight) mice were treated with single dose of 10 Gy gamma-ray at a rate of 1.0 Gy/min total abdominal irradiation. Animal body weight was assessed per five days.

2.3. Morris water maze tests

The Morris water maze tests are used to evaluate spatial reference learning and memory of mice. In this study, a circular water tank (120 cm diameter, 25 ± 1 °C) with hidden quadrants was used and the surrounding was decorated with eye-catching visual cues to orient subjected mice. A clear 12 cm (diameter) escape platform was placed 1.5 cm below the water surface, which was made opaque with white non-toxic tempera paint. The quadrant containing the platform refers to the target zone. Hidden platform test was performed for 5 days. Irradiated mice were trained for 5 consecutive days with 4 trials per day as acquisition trials from the next day after irradiation. Each trial began with placing the mouse into a different quadrant and allowing it to swim freely for a maximum period (60 s). After each mouse reached the platform (or were guided to the platform if mice were unable to locate the platform after 30 s), they were returned to their home cage to dry for 10 min. The time taken to reach the platform of each mouse refers to escape latency. On the 6 day, probe test was performed to determine memory retention without the platform for 60 s. Each mouse was placed into the opposite quadrant of the target zone where the platform was removed (time in the target zone), n = 18 (or 12) per group. Data were recorded and analyzed using a video camera-based Ethovision System (Nodulus, The Netherlands).

2.4. Cell culture

The 3T3 cells were maintained in DMEM (Gibco). The cells were supplemented with heat-inactivated 10% FBS (Gibco), 100 U/mL penicillin, and 100 mg/mL streptomycin and grown at 5% CO_2 and 37 °C.

2.5. Plasmid construction

Two ~ 300 bp fragment of *Bdnf* 3′UTR was subcloned into pGL3-control vector (Promega, Madison, WI USA) immediately downstream of the stop codon of the luciferase gene to generate pGL3-*Bdnf*-2427 and pGL3-*Bdnf*-2020. Mutant construct of conserved seed region of *Bdnf* 3′UTR (named as pGL3-*Bdnf*-2427-mut and pGL3-*Bdnf*-2020-mut), carrying a substitution of nucleotides within the core seed sequence of miR-34a-5p, was conducted using overlapping extension PCR. The primers were listed in Supplementary Table S1.

2.6. Cell transfection

The cells were cultured in a 6-well or 24-well plate for 24 h and then were transfected with miRNA and plasmids. All transfections were performed using Lipofectamine 2000 reagent (Invitrogen, Carlsbad, CA, USA) according to the manufacturer's protocol. miR-34a-5p and anti-miR-34a-5p were synthesized by RiboBio (Guangzhou, China).

2.7. Luciferase reporter assays

Luciferase reporter assays were performed using the Dual-Luciferase Reporter Assay System (Promega, Madison, WI, USA) according to the manufacturer's instructions. Cells were cultured in 24-well plates with about 3×10^4 cells per well. After 24 h, the cells were transiently co-transfected with the pRL-TK plasmid (Promega, Madison, WI, USA) containing the *Renilla* luciferase gene, which is used for internal normalization, and with construct carrying seed sequence of 3′UTR of *Bdnf* (or pGL3-control). All experiments were performed at least three times.

2.8. Western blotting analysis

The expression of *Bdnf* was examined using Western blotting analysis. Ice-cold radio-immuno-precipitation assay (RIPA) buffer supplemented with phosphatase and protease inhibitors was used for protein extraction. Total protein samples were filtered *via* SDS-PAGE (Polyacrylamide Gel Electrophoresis) (12% acrylamide gel) using the Bio-Rad Trans-Blot system and were transferred to membranes. The primary antibodies used were mouse anti-β-actin (Sigma, St Louis, MO) and rabbit anti-BDNF (Proteintech Group, Chicago, IL). All experiments were repeated at least three times.

2.9. Tail vein injection

One hundred μl DEPC water dissolved 0.5 μM miR-34a-5p antagomir was introduced by tail vein injection immediately after TAI. DEPC water with negative control was administrated as control. Morris water maze tests were performed following the aforementioned protocol. miR-34a-5p antagomir and negative control were synthesized by RiboBio (Guangzhou, China). The tail vein injection performed at the next day after TAI exposure, n = 12 per group.

2.10. Quantitative real-time polymerase chain reaction (qRT-PCR)

Total RNA was separated from mouse tissues using Trizol (Invitrogen, Carlsbad, CA, USA) according to the manufacturer's protocol. For mature miR-34a-5p detection, total RNA was polyadenylated by poly(A) polymerase (Ambion, Austin, TX, USA) as described previously [21]. cDNA was produced by using poly(A)-tailed total RNA and reverse transcription primer with ImProm-IIReverse Transcriptase (Promega, Madison, WI, USA), according to the manufacturer's instructions. The qRT-PCR was performed according to the instructions of Fast Start Universal SYBR Green Master (Rox) (Roche Diagnostics GmbH Mannheim, Germany). The primers used in this study were listed in Supplementary Table S1.

2.11. Bacterial diversity analysis

Stool samples were freshly collected and stored at − 80 °C before used. DNA was extracted from the stool using a Power Fecal® DNA Isolation Kit (MoBio Carlsbad, CA USA). The DNA was recovered with 30 mL of buffer in the Kit. The 16S ribosomal RNA (rRNA) gene was analyzed to evaluate the bacterial diversity by using Illumina Hiseq (Novogene Bioinformatics Technology Co., Ltd.), n = 5 per group. The primers are listed in Supplementary Table 1.

2.12. Microarray analysis

The mice were euthanized and the small intestine tissues were excised at day 7 after TAI exposure. These samples were used to synthesize double-stranded complementary DNA (cDNA) and the cDNA was labeled and hybridized to Affymetrix genechip microarray 4.0 (CapitalBio Corp., Beijing, China) according to the manufacturer's instructions. The data from microarray were used to analyze data summarization, normalization and quality control using the Gene Spring software V11.5 (Agilent). The differentially expressed microRNA were selected if the change of threshold values were > 2.0-fold and if Benjamini-Hochberg corrected *P* values were < 0.05. The data were normalized and hierarchically clustered with CLUSTER 3.0 software. The data were performed the visualization with Java Tree view software.

2.13. Inflammatory cytokines analysis

For serum IL-6 and TNF-α levels measurement, the irradiated mice were euthanized at day 7 after TAI exposure. Serum levels of IL-6 and TNF-α (Beijing Solarbio Science & Technology, Beijing, China) were quantified using ELISA according to manufacturer's instructions.

For quantification of faecal LCN2, frozen faecal samples were reconstituted in saline containing 0.1% Tween 20 to a final concentration of 100 mg/mL and vortexed for 20 min to produce a homogenous faecal suspension. These samples were then centrifuged for 10 min at 14,000*g* and 4 °C. Clear supernatants were collected and stored at − 80 °C. LCN2 levels were assessed in the supernatants using Duoset murine LCN2 ELISA kit (R&D Systems, Minneapolis, Minnesota) according to manufacturer's instructions.

2.14. Donor stool preparation and administration

The healthy 6- to 8-week-old female C57BL/6 mice were kept in same housing and environmental conditions. Conventional, untreated, age-matched female were used as donors to collect gut microbiota. Donor stool was freshly prepared on the day of transplant and that in all cases was prepared and transplanted within 4 h. Donor stool pellets were weighed and diluted with 1 mL of saline per 100 mg of stool. Briefly, the stool was steeped in saline for about 15 min, shaken and then centrifuged at 800 rpm for 3 min. The supernatant was obtained for treatment. The mice in each group were treated with same sample. The recipients were 12 per group.

2.15. Statistical analysis

The data are presented as the means ± SEM with respect to the number of samples (n) in each group. Statistical significance between multiple treatment groups was determined by analysis of variance (ANOVA) and Student *t*-test. The survival rates were analyzed using the Kaplan–Meier survival test. Results with $P < 0.05$ were considered statistically significant.

3. Results

3.1. Total abdominal irradiation induces cognitive deficits in mouse models

To investigate the effect of TAI on cognitive function, we performed Morris water maze (MWM) test to assess animals' spatial learning and memory (Fig. 1A). Following exposure to total abdominal irradiation (gamma-ray, 10 Gy), mice exhibited radiation-induced alopecia (hair loss) after 2 months (Fig. 1B), confirming that TAI indeed induced abdominal injury. With progressive task training, the escape latency time to find the platform was progressively reduced for both healthy control and TAI-challenged mice (Fig. 1C). At day 5, animals from TAI group spent significant more time to find the platform than healthy controls (Fig. 1C), whereas there was no apparent difference in the body size (Supplementary Fig. 1A), swimming speed (Fig. 1D) and body weight (Fig. 1E) between these two cohorts. At day 6, the TAI-exposed mice spent about 40% less time swimming in the target quadrant than controls (Fig. 1F and Supplementary Fig. 1B), although nuclear magnetic resonance analysis did not reveal overt difference in structure of the brain between these mice (Supplementary Fig. 1C). We further validated that TAI exposure did not alter the levels of *IL-6* and *TNF-α* in peripheral blood (Fig. 1G, H), suggesting that irradiated animals did not have abnormal immunity or low-graded systemic inflammation.

3.2. TAI divergently modulates the expression of miR-34a-5p and *Bdnf*

To decipher the underlying mechanism of TAI-induced cognitive impairment, we compared expression profiles of various miRNAs in small intestine tissues between healthy control and TAI-exposed mice. As expected, the expression levels of many miRNAs were altered ($P < 0.05$, moderated *t*-test with Benjamini-Hochberg multiple testing correction, > 2-fold change; Fig. 2A). For instance, bioinformatics analysis (microrna.org, http://www.microrna.org//microrna/home.do) revealed a marked elevation of miR-34a-5p, which can potentially target a number of genes including BDNF (Supplementary Fig. 2), which is an indispensable neurotrophic factor engaging in intricate cerebral functions [22].

Quantitative real-time polymerase chain reaction (qRT-PCR) analysis further confirmed the increase of miR-34a-5p in small intestine tissues and peripheral blood from TAI treated mice compared with healthy controls (Fig. 2B, C). Given the essential role of BDNF in brain function, we compared the expression level of miR-34a-5p in the hippocampus between TAI-exposed and control mice. Interestingly, the hippocampal miR-34a-5p level was about 2.5-fold higher in TAI-challenged mice than those of healthy controls (Fig. 2D), and appeared to be inversely correlated with the hippocampal expression of *Bdnf* mRNA (Fig. 2E). The decrease of hippocampal *Bdnf*mRNA and protein expression in TAI-challenged mice was further validated by qRT-PCR and Western blotting analyses (Fig. 2F, G). ELISA and qRT-PCR analyses exhibited that irradiated mice carried higher levels of faecal *LCN2* and small intestinal *IL-6* comparing with the healthy control (Fig. 2H, I), suggesting that TAI exposure might cause gut inflammation in mouse models.

To further nail the relationship between miR-34a-5p and *Bdnf*, we constructed plasmids, pGL3-Bdnf (2427) and pGL3-Bdnf (2020), carrying the two potential binding sites for miR-34a-5p in the 3′UTR of *Bdnf* mRNA (Fig. 3A, B). Luciferase reporter assays revealed that miR-34a-5p directly bound to the seed regions, but failed to influence the paired seed region mutants (pGL3-Bdnf (2427)-mut and pGL3-Bdnf (2020)-mut) (Fig. 3C and Supplementary Fig. 3A). Conversely, anti-miR-34a-5p increased the luciferase activities of both plasmids rather than the paired mutants (Fig. 3D and Supplementary Fig. 3B), suggesting that miR-34a-5p directly binds to the 3′UTR of *Bdnf* mRNA. Furthermore, the enforced expression of miR-34a-5p resulted in a counter-regulation of *Bdnf* expression in 3 T3 cells in a dose-dependent fashion (Fig. 3E), which was repeatable by treating the cells with anti-miR-34a-5p (Fig. 3F).

3.3. Tail intravenous injection of miR-34a-5p antagomir ameliorates TAI-induced cognitive dysfunction through restoring *Bdnf* expression in the hippocampus

To further elaborate the role of miR-34a-5p in TAI-induced cognitive deficits, we intravenously injected miR-34a-5p antagomir immediately following TAI. The administration of miR-34a-5p antagomir erased TAI-elevated miR-34a-5p in the peripheral blood (Fig. 4A), as well as in the hippocampus (Fig. 4B). Moreover, peripheral administration of miR-34a-5p antagomir also significantly restored *Bdnf* expression in hippocampus (Fig. 4C, D).

To test whether miR-34a-5p antagomir could mitigate TAI-impaired cognition, we performed MWM tests in parallel experiments. Although the escape latency to find the platform was continuously lessened from day 1 to day 4 of training for all cohorts, at day 5 the time wasted by TAI mice to find the platform was significant longer than both of another two cohorts (Fig. 4E). There was no significant difference in the swimming speed between different groups (Supplementary Fig. 4A) however, the TAI-induced shortening of sequestered time in the target quadrant was almost completely restored by administration of miR-34a-5p antagomir (Fig. 4F, Supplementary Fig. 4B). Notably, tail vein injection of miR-34a-5p antagomir erased TAI-heightened faecal *LCN2* and small intestinal *IL-6* (Fig. 4G, H), suggesting that injection of miR-34a-5p antagomir might mitigate TAI-caused gut inflammation.

3.4. Tail intravenous injection of miR-34a-5p antagomir shapes the intestinal bacterial composition after TAI

Given gut–brain crosstalk generates a sophisticated, bidirectional communication system that has multiple effects on motivation and higher cognitive functions [23] and gut bacteria can alter host's behavior and potentially drive the onset and/or severity of nervous system disorders [24], we examined the shift of gut microbiota mediated by TAI. The observed species and Shannon index analysis showed none significant alteration of gut microbiota in mice after TAI exposure (Fig. 5A, C); however, miR-34a-5p antagomir injection changed the enteric bacterial composition at day 3 post irradiation (Fig. 5B, D). As the genus level, top 10 harbored bacteria in irradiated mice with or without miR-34a-5p antagomir injection was different (Fig. 5E, F). In detail, TAI decrease the frequency of *Helicobacter* and unchanged that of *Lactobacillus* (Fig. 5E, Supplementary Fig. 5A). But miR-34a-5p antagomir injection stabled the frequency of *Helicobacter* and increased that of *Lactobacillus* at day 3 in irradiated mice (Fig. 5F, Supplementary Fig. 5B). Given faecal miRNA-mediated inter-species gene regulation facilitates host control of the gut microbiota [25], the principal component analysis (PCA) and Beta diversity analysis showed that the gut bacterial composition profile did not overtly shift after TAI exposure at day 6 in mice with or without miR-34a-5p antagomir injection (Fig. 6A–D); however, at phylum level and in detail, the irradiation-altered frequency of Bacteroidetes and Firmicutes (Fig. 6E, F) was almost completely restored back to the normal level at day 6 following administration of miR-34a-5p antagomir, suggesting that administration of exogenous miRNA might retain the enteric bacterial community. MyD88 has been reported to mediate gut microbiota dynamics [26], and bioinformatics analysis showed miR-34a-5p has potential to bind to the mRNA of MyD88 (microrna.org, http://www.microrna.org//microrna/home.do). Thus, we assessed the expression level of *MyD88* in small intestine tissues and observed that TAI exposure reduced the level of *MyD88*, but tail veil injection of miR-34a-5p antagomir erased the events (Fig. 6G), suggesting that *MyD88*might be involved in retaining TAI-shifted gut microbiota mediated by injection of miR-34a-5p antagomir.

To better understand the effect of gut microbiota on TAI-impaired cognitive function, we transplanted enteric microbes from TAI-challenged mice with or without tail veil injection of miR-34a-5p to recipients (Supplementary Fig. 6). MWM test showed that the escape latency to find the platform was continuously lessened from day 1 to day 5 of training for all cohorts (Fig. 6H), however, the mice carried gut microbes from donors with TAI exposure spent less sequestered time in the target quadrant comparing with that of control and mice transplanted gut microbes from irradiated mice with miR-34a-5p antagomir injection (Fig. 6I), suggesting that gut microbiota might be involved in TAI-impaired cognitive function.

4. Discussion

As a popular cancer therapeutic approach, radiotherapy kills both cancer cells and bystander normal cells, thereby remarkably affecting the integrity and function of healthy tissues [27]. Recently, wealth of clinical studies support the notion that radiotherapy-mediated side effects remain a conundrum, intertwined with impaired life quality of survivors. In detail, telangiectasia and fibrosis occur as late skin side effects, and therapy-associated

cardiovascular disease from breast carcinoma patients performed breast-conserving surgery followed by radiotherapy [28] ; [29]. Sophisticated oral sequelae, such as mucositis and salivary hypofunction, occur following radiotherapy toward head and neck cancer [30] ; [31]. Radiotherapy-induced bowel/bladder toxicity affects the life quality of patients with prostate cancer [32]. Acute inflammatory accompanying with pelvic malignancy radiotherapy causes gastrointestinal symptoms during treatment [33] and, cranial irradiation leads to long-lasting cognitive impairments in patients receiving radiotherapy for the treatment of malignant brain tumors [34]. Given central nervous system (CNS) responds to the stimuli from gut [35], we performed Morris water maze test to examine the effect of total abdominal irradiation on cognition using mouse models. Our observations showed that TAI exposure caused cognitive deficits in mouse models, indicating that peripheral organs exposed to irradiation might adversely impair the function of central nervous system.

A significant barrier of CNS is the blood–brain barrier (BBB), which prevents large or hydrophilic molecules such as dopamine, chemotherapeutics, and viruses from passively entering the brain [36]. However, peripheral changes of miRNAs is associated with psychiatric illness [37], suggesting that circulating miRNAs affect the function of brain. Thus, we focused on miRNAs to interrogate the molecular mechanism by which TAI subverted cognition. Intriguingly, total abdominal irradiation up-regulated the level of miR-34a-5p in the small intestine, peripheral blood as well as hippocampus, resulting in the down-regulation of *Bdnf* in hippocampus through targeting its 3′UTR, indicating that miR-34a-5p/BDNF axis might be involved in TAI-induced cognitive deficits. To further validate the conjecture, we injected miR-34a-5p antagomir from vein tail into the mice immediately after TAI. As expected, miR-34a-5p antagomir injection prevented the TAI-mediated elevation of miR-34a-5p in peripheral blood and hippocampus, restored the expression of *Bdnf* in hippocampus and cognitive function of TAI mice. On the basis of bioinformatics analysis, other genes might be targeted by miR-34a-5p, such as *Wnt5a*, *Notch1* and *Stat3*, could also be involved in the development of memory formation or neuron functionality, which required further studied. Collectively, our findings bolster that miR-34a-5p might be served as a biomarker to diagnose the side effects engendered by radiotherapy toward abdominal and pelvic cancer. What is more, miR-34a-5p and *Bdnf*might be employed as potential therapeutic targets to ameliorate radiotherapy induced side effects.

With an estimated composition of 100 trillion cells, the human body is home to microorganisms far more than human cells, among which are typically dominated by bacteria co-developing with the host from birth [38]; [39] ; [40]. Mounting emerging evidence delineate that microbially produced molecule can get absorbed into the bloodstream, infiltrate the blood-brain barrier and impact the behavior and cognition of host [41]. Intestinal microbiota communicates with the brain to influence neurological outcomes —altering behaviors and potentially affecting the onset and/or severity of nervous system disorders [18]; [24] ; [42]. Thus, we obtained that TAI exposure shifted the composition of enteric bacteria progressively, indicating that intestinal bacteria might participate in TAI-induced cognitive deficits. Recent investigation reveal that treatment of adult mice with antibiotics decreases hippocampal neurogenesis and memory retention [43], further validating the effect of gut bacteria on the cognitive function of host. Epidemiological studies and animal models support Parkinson disease seems to start from the enteric nervous

system and further into the CNS, intestinal microbiota seems to be involved in this process [44]. Inspired by the studies, we are inquisitive whether miR-34a-5p antagomir recuperates the cognition *via* restoring the intestinal bacterial community shifted by TAI. High throughput sequencing analysis showed that tail intravenous injection of miR-34a-5p antagomir retained the profile of intestinal bacteria of total abdominal irradiated mice, indicating that exogenous miRNAs alter the intestinal bacterial community as well. Myd88 and gut inflammation have been reported to be involved in gut microbiota dynamics. Thus, we measured the expression level of small intestinal *MyD88* and gut microbiota in our system. Intriguingly, TAI exposure elevated the level of intestinal *MyD88* and caused gut inflammation in mouse models, but tail vein injection of miR-34a-5p antagomir erased the events, suggesting that *MyD88* and gut microbiota are implicated in miR-34a-5p antagomir retained gut microbiota shifted by TAI. Our observation implied that intestinal microbiota retained might be an essential event during the therapy and it might be a novel therapeutic scheme.

In summary, our work demonstrates that total abdominal irradiation causes cognitive impairment in mouse models. TAI up-regulates miR-34a-5p in small intestine and peripheral blood, which down-regulates the expression of *Bdnf* through targeting its 3′UTR in hippocampus. Tail intravenous injection of miR-34a-5p antagomir inhibits the increase of miR-34a-5p in peripheral blood and hippocampus, recovers the cognitive dysfunction. In addition, miR-34a-5p antagomir injection retains the TAI-altered intestinal bacterial composition pattern. Thus, our findings provide new insights into the side effects of radiotherapy toward abdominal and pelvic cancer and unravel the underling mechanism.

Supplementary Material

Refer to Web version on PubMed Central for supplementary material.

Acknowledgments

We thank Prof. Zhuo Yang (College of Medicine, Nankai University) for guiding us to perform Morris water maze test. This work was supported by grants from the National Natural Science Foundation of China (No. 81502664, 81172127 and 81402541), the Technology and Development and Research Projects for Research Institutes, Ministry of Science and Technology (2014EG150134), the TJKJZC (14ZCZDSY00001), the PUMC Youth Fund and the Fundamental Research Funds for the Central Universities (No. 33320140187), the IRM-CAMS Research Fund (No. 1547 and 1522). H.W. is supported by the U.S. National Center of Complementary and Alternative Medicine (NCCAM, R01AT005076) and the National Institute of General Medical Sciences (NIGMS, R01GM063075).

References

1. Drew DA, Cao Y, Chan AT. Aspirin and colorectal cancer: the promise of precision chemoprevention. Nat Rev Cancer. 2016; 16:173–186. [PubMed: 26868177]
2. Tarish FL, Schultz N, Tanoglidi A, Hamberg H, Letocha H, Karaszi K, Hamdy FC, Granfors T, Helleday T. Castration radiosensitizes prostate cancer tissue by impairing DNA double-strand break repair. Sci Transl Med. 2015; 7:312re311.
3. Xie Y, Shen YT, Kapoor A, Ojo D, Wei F, De Melo J, Lin X, Wong N, Yan J, Tao L, Major P, Tang D. CYB5D2 displays tumor suppression activities towards cervical cancer. Biochim Biophys Acta. 2016; 1862:556–565. [PubMed: 26692170]
4. Barker HE, Paget JT, Khan AA, Harrington KJ. The tumour microenvironment after radiotherapy: mechanisms of resistance and recurrence. Nat Rev Cancer. 2015; 15:409–425. [PubMed: 26105538]

5. Mukherjee D, Coates PJ, Lorimore SA, Wright EG. Responses to ionizing radiation mediated by inflammatory mechanisms. J Pathol. 2014; 232:289–299. [PubMed: 24254983]
6. Bentzen SM. Preventing or reducing late side effects of radiation therapy: radiobiology meets molecular pathology. Nat Rev Cancer. 2006; 6:702–713. [PubMed: 16929324]
7. Weigel C, Veldwijk MR, Oakes CC, Seibold P, Slynko A, Liesenfeld DB, Rabionet M, Hanke SA, Wenz F, Sperk E, Benner A, Rosli C, Sandhoff R, Assenov Y, Plass C. Epigenetic regulation of diacylglycerol kinase alpha promotes radiation-induced fibrosis. Nat Commun. 2016; 7:10893. [PubMed: 26964756]
8. Paris F, Fuks Z, Kang A, Capodieci P, Juan G, Ehleiter D, Haimovitz-Friedman A, Cordon-Cardo C, Kolesnick R. Endothelial apoptosis as the primarylesion initiating intestinal radiation damage in mice. Science. 2001; 293:293–297. [PubMed: 11452123]
9. Park H, Poo MM. Neurotrophin regulation of neural circuit development and function. Nat Rev Neurosci. 2013; 14:7–23. [PubMed: 23254191]
10. Liao GY, An JJ, Gharami K, Waterhouse EG, Vanevski F, Jones KR, Xu B. Dendritically targeted Bdnf mRNA is essential for energy balance and response to leptin. Nat Med. 2012; 18:564–571. [PubMed: 22426422]
11. Zuccato C, Cattaneo E. Brain-derived neurotrophic factor in neurodegenerative diseases. Nat Rev Neurol. 2009; 5:311–322. [PubMed: 19498435]
12. Gerenu, G., Martisova, E., Ferrero, H., Carracedo, M., Rantamäki, T., Ramirez, M., Gil-Bea, FJ. Modulation of BDNF cleavage by plasminogen-activator inhibitor-1 contributes to Alzheimer's neuropathology and cognitive deficits; Biochim Biophys Acta. 2017 Jan 26. p. 30036-4http://dx.doi.org/10.1016/j.bbadis.2017.01.023 (pii: S0925-4439, Epub ahead of print).
13. Cui M, Wang Y, Sun B, Xiao Z, Ye L, Zhang X. MiR-205 modulates abnormal lipid metabolism of hepatoma cells via targeting acyl-CoA synthetase long-chain family member 1 (ACSL1) mRNA. Biochem Biophys Res Commun. 2014; 444:270–275. [PubMed: 24462768]
14. Li X, Khanna A, Li N, Wang E. Circulatory miR34a as an RNAbased, noninvasive biomarker for brain aging. Aging. 2011; 3:985–1002. [PubMed: 22064828]
15. Zhang, QJ., Li, J., Zhang, SY. Effects of TRPM7/miR-34a gene silencing on spatial cognitive function and hippocampal neurogenesis in mice with type 1 diabetes mellitus. Mol Neurobiol. 2017 Feb 9. http://dx.doi.org/10.1007/s12035-017-0398-5 Epub ahead of print
16. Mayer EA, Labus JS, Tillisch K, Cole SW, Baldi P. Towards a systems view of IBS. Nat Rev Gastroenterol Hepatol. 2015; 12:592–605. [PubMed: 26303675]
17. Eisenstein M. Microbiome: bacterial broadband. Nature. 2016; 533:S104–S106. [PubMed: 27191486]
18. Cryan JF, Dinan TG. Mind-altering microorganisms: the impact of the gut microbiota on brain and behaviour. Nat Rev Neurosci. 2012; 13:701–712. [PubMed: 22968153]
19. De Vadder F, Kovatcheva-Datchary P, Goncalves D, Vinera J, Zitoun C, Duchampt A, Backhed F, Mithieux G. Microbiota-generated metabolites promote metabolic benefits via gut-brain neural circuits. Cell. 2014; 156:84–96. [PubMed: 24412651]
20. Cui M, Xiao H, Luo D, Zhang X, Zhao S, Zheng Q, Li Y, Zhao Y, Dong J, Li H, Wang H, Fan S. Circadian rhythm shapes the gut microbiota affecting host radiosensitivity. Int J Mol Sci. 2016; 17:11. pii: E1786.
21. Cui M, Xiao Z, Wang Y, Zheng M, Song T, Cai X, Sun B, Ye L, Zhang X. Long noncoding RNA HULC modulates abnormal lipid metabolism in hepatoma cells through an miR-9-mediated RXRA signaling pathway. Cancer Res. 2015; 75:846–857. [PubMed: 25592151]
22. Li M, Armelloni S, Zennaro C, Wei C, Corbelli A, Ikehata M, Berra S, Giardino L, Mattinzoli D, Watanabe S, Agostoni C, Edefonti A, Reiser J, Messa P, Rastaldi MP. BDNF repairs podocyte damage by microRNA-mediated increase of actin polymerization. J Pathol. 2015; 235:731–744. [PubMed: 25408545]
23. Mayer EA. Gut feelings: the emerging biology of gut-brain communication. Nat Rev Neurosci. 2011; 12:453–466. [PubMed: 21750565]
24. Sampson TR, Mazmanian SK. Control of brain development, function, and behavior by the microbiome. Cell Host Microbe. 2015; 17:565–576. [PubMed: 25974299]

25. Liu S, da Cunha AP, Rezende RM, Cialic R, Wei Z, Bry L, Comstock LE, Gandhi R, Weiner HL. The host shapes the gut microbiota via fecal microRNA. Cell Host Microbe. 2016; 19:32–43. [PubMed: 26764595]
26. Heimesaat MM, Nogai A, Bereswill S, Plickert R, Fischer A, Loddenkemper C, Steinhoff U, Tchaptchet S, Thiel E, Freudenberg MA, Gobel UB, Uharek L. MyD88/TLR9 mediated immunopathology and gut microbiota dynamics in a novel murine model of intestinal graft-versus-host disease. Gut. 2010; 59:1079–1087. [PubMed: 20639251]
27. Liu X, Cotrim A, Teos L, Zheng C, Swaim W, Mitchell J, Mori Y, Ambudkar I. Loss of TRPM2 function protects against irradiation-induced salivary gland dysfunction. Nat Commun. 2013; 4:1515. http://dx.doi.org/10.1038/ncomms2526. [PubMed: 23443543]
28. Chang-Claude J, Ambrosone CB, Lilla C, Kropp S, Helmbold I, von Fournier D, Haase W, Sautter-Bihl ML, Wenz F, Schmezer P, Popanda O. Genetic polymorphisms in DNA repair and damage response genes and late normal tissue complications of radiotherapy for breast cancer. Br J Cancer. 2009; 100:1680–1686. [PubMed: 19367277]
29. Zagar TM, Cardinale DM, Marks LB. Breast cancer therapy-associated cardiovascular disease. Nat Rev Clin Oncol. 2016; 13:172–184. [PubMed: 26598943]
30. Ray-Chaudhuri A, Shah K, Porter RJ. The oral management of patients who have received radiotherapy to the head and neck region. Br Dent J. 2013; 214:387–393. [PubMed: 23619856]
31. van Luijk P, Pringle S, Deasy JO, Moiseenko VV, Faber H, Hovan A, Baanstra M, van der Laan HP, Kierkels RG, van der Schaaf A, Witjes MJ, Schippers JM, Brandenburg S, Langendijk JA, Wu J, Coppes RP. Sparing the region of the salivary gland containing stem cells preserves saliva production after radiotherapy for head and neck cancer. Sci Transl Med. 2015; 7:305ra147.
32. Dearnaley DP, Hall E, Lawrence D, Huddart RA, Eeles R, Nutting CM, Gadd J, Warrington A, Bidmead M, Horwich A. Phase III pilot study of dose escalation using conformal radiotherapy in prostate cancer: PSA control and side effects. Br J Cancer. 2005; 92:488–498. [PubMed: 15685244]
33. McGough C, Baldwin C, Frost G, Andreyev HJ. Role of nutritional intervention in patients treated with radiotherapy for pelvic malignancy. Br J Cancer. 2004; 90:2278–2287. [PubMed: 15162154]
34. Belarbi K, Jopson T, Arellano C, Fike JR, Rosi S. CCR2 deficiency prevents neuronal dysfunction and cognitive impairments induced by cranial irradiation. Cancer Res. 2013; 73:1201–1210. [PubMed: 23243025]
35. Murphy KG, Bloom SR. Gut hormones and the regulation of energy homeostasis. Nature. 2006; 444:854–859. [PubMed: 17167473]
36. Yang B, Li S, Wang H, Guo Y, Gessler DJ, Cao C, Su Q, Kramer J, Zhong L, Ahmed SS, Zhang H, He R, Desrosiers RC, Brown R, Xu Z, Gao G. Global CNS transduction of adult mice by intravenously delivered rAAVrh.8 and rAAVrh.10 and nonhuman primates by rAAVrh.10. Mol Ther. 2014; 22:1299–1309. [PubMed: 24781136]
37. Scott KA, Hoban AE, Clarke G, Moloney GM, Dinan TG, Cryan JF. Thinking small: towards microRNA-based therapeutics for anxiety disorders. Expert Opin Investig Drugs. 2015; 24:529–542.
38. Gomez de Aguero M, Ganal-Vonarburg SC, Fuhrer T, Rupp S, Uchimura Y, Li H, Steinert A, Heikenwalder M, Hapfelmeier S, Sauer U, McCoy KD, Macpherson AJ. The maternal microbiota drives early postnatal innate immune development. Science. 2016; 351:1296–1302. [PubMed: 26989247]
39. Cenit MC, Matzaraki V, Tigchelaar EF, Zhernakova A. Rapidly expanding knowledge on the role of the gut microbiome in health and disease. Biochim Biophys Acta. 2014; 1842:1981–1992. [PubMed: 24882755]
40. Cui M, Xiao H, Li Y, Zhou L, Zhao S, Luo D, Zheng Q, Dong J, Zhao Y, Zhang X, Zhang J, Lu L, Wang H, Fan S. Faecal microbiota transplantation protects against radiation-induced toxicity. EMBO Mol Med. 2017; 9:448–461. [PubMed: 28242755]
41. Fischbach MA, Segre JA. Signaling in host-associated microbial communities. Cell. 2016; 164:1288–1300. [PubMed: 26967294]
42. Collins SM, Surette M, Bercik P. The interplay between the intestinal microbiota and the brain. Nat Rev Microbiol. 2012; 10:735–742. [PubMed: 23000955]

43. Möhle L, Mattei D, Heimesaat Markus M, Bereswill S, Fischer A, Alutis M, French T, Hambardzumyan D, Matzinger P, Dunay Ildiko R, Wolf Susanne A. Ly6C(hi) monocytes provide a link between antibiotic-induced changes in gut microbiota and adult hippocampal neurogenesis. Cell Rep. 2016; 15:1945–1956. [PubMed: 27210745]

44. Klingelhoefer L, Reichmann H. Pathogenesis of Parkinson disease—the gut-brain axis and environmental factors. Nat Rev Neurol. 2015; 11:625–636. [PubMed: 26503923]

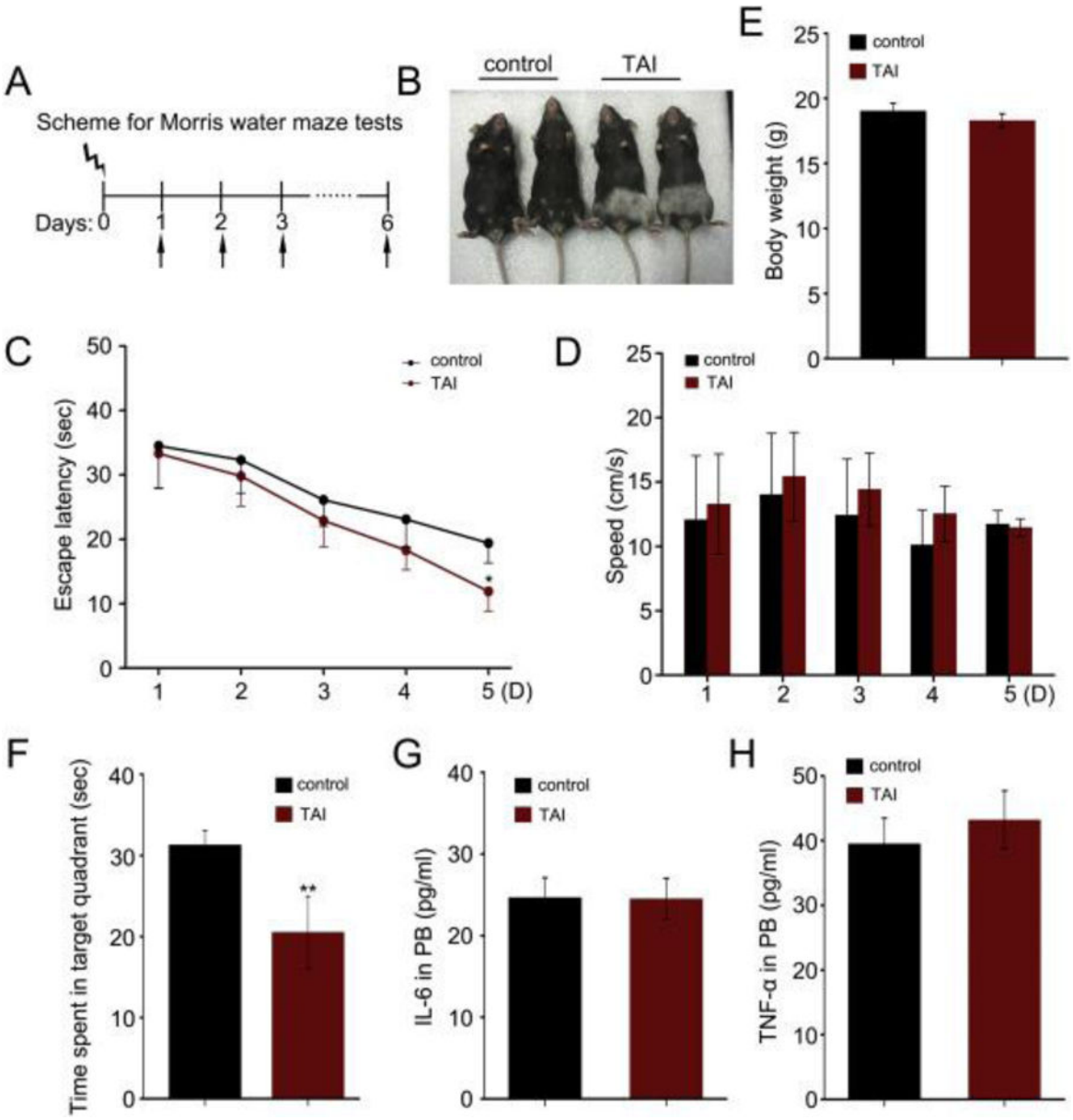

Figure 1. Total abdominal irradiation impairs cognitive function in mouse models

(A) Scheme for Morris water maze test. (B) The mice exposed to 10 Gy TAI (right) along with mice without irradiation (left). Note the change in fur color in the irradiated lower body. (C, D) The escape latency time to reach the hidden platform and swimming speed during the 5 days of Morris water maze test were shown. $F_{(1, 71)} = 4.381$, $^{*}P < 0.05$, ANOVA, n = 18. (E) The body weight of mice with or without TAI was measured. (F) The times spent in target quadrant and swimming traces in 60 s at day 6 of Morris water maze were shown. $F_{(1, 17)} = 9.072$, $^{**}P < 0.01$, ANOVA, n = 18. (G, H) The levels of IL-6 (G) and TNF-α (H) in peripheral blood were examined by ELISA. No significant difference; Student *t*-test, n = 18.

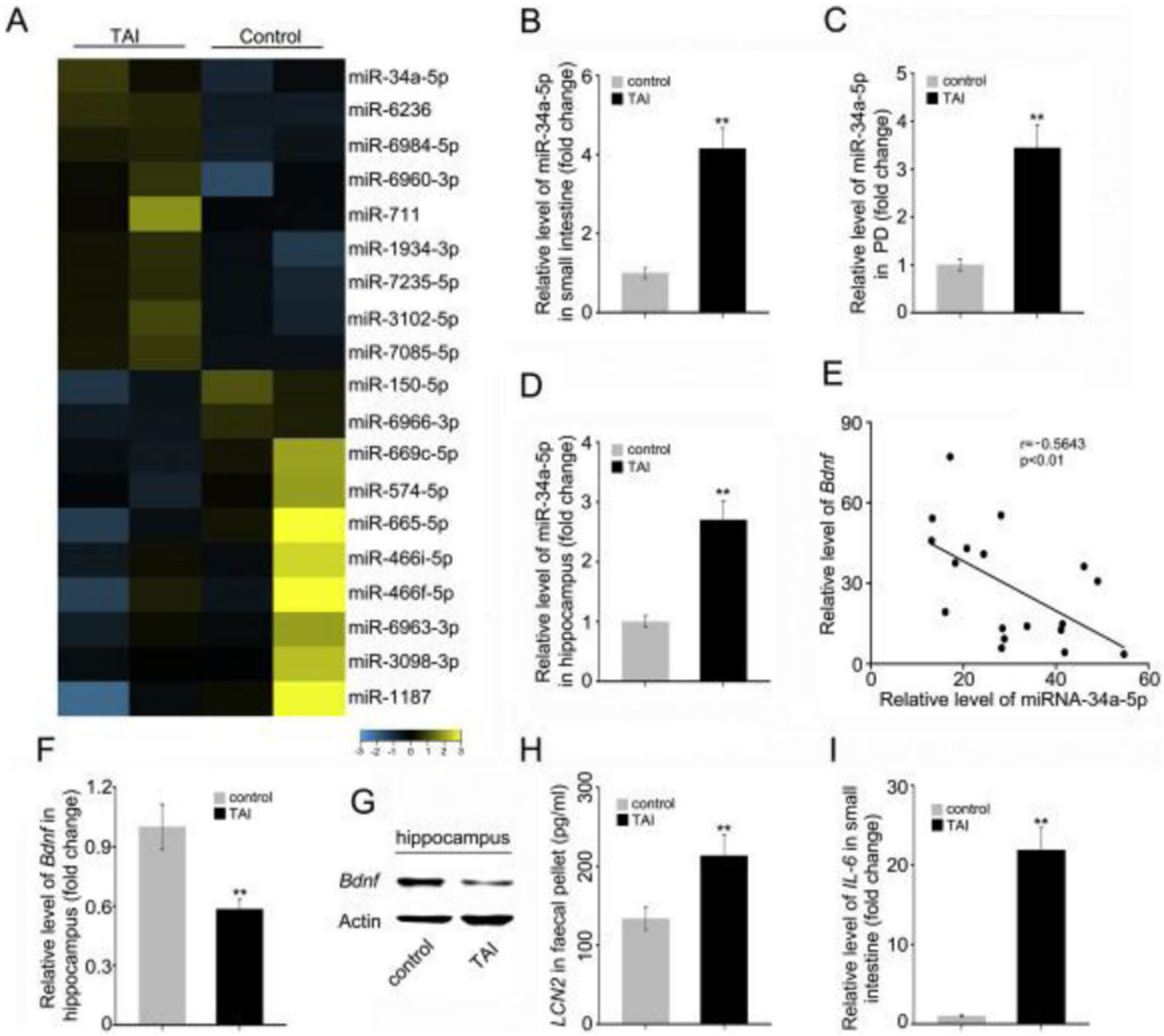

Figure 2. TAI exposure causes up-regulation of miR-34a-5p and parallel down-regulation of *Bdnf*

(A) Microarray analysis was performed using small intestine tissues from mice with or without TAI. (B–D) The levels of miR-34a-5p in small intestine (B), PB (C) and hippocampus (D) were assessed by qRT-PCR. (E) The correlation between *Bdnf* mRNA and miR-34a-5p level was examined by qRT-PCR in 18 cases of hippocampus tissues from TAI exposed mice ($P < 0.01$; Pearson correlation coefficient, $r = -0.5643$). (F, G) The mRNA and protein levels of *Bdnf* were assessed by qRT-PCR and Western blotting in hippocampus from mice with or without TAI. (H) The level of faecal *LCN2* was measured by ELISA from mice with or without TAI. (I) The mRNA level of *IL-6* in small intestine tissues was examined by qRT-PCR from mice with or without TAI. Statistically significant differences are indicated: $^{**}P < 0.01$; Student *t*-test, n = 18 mice/group.

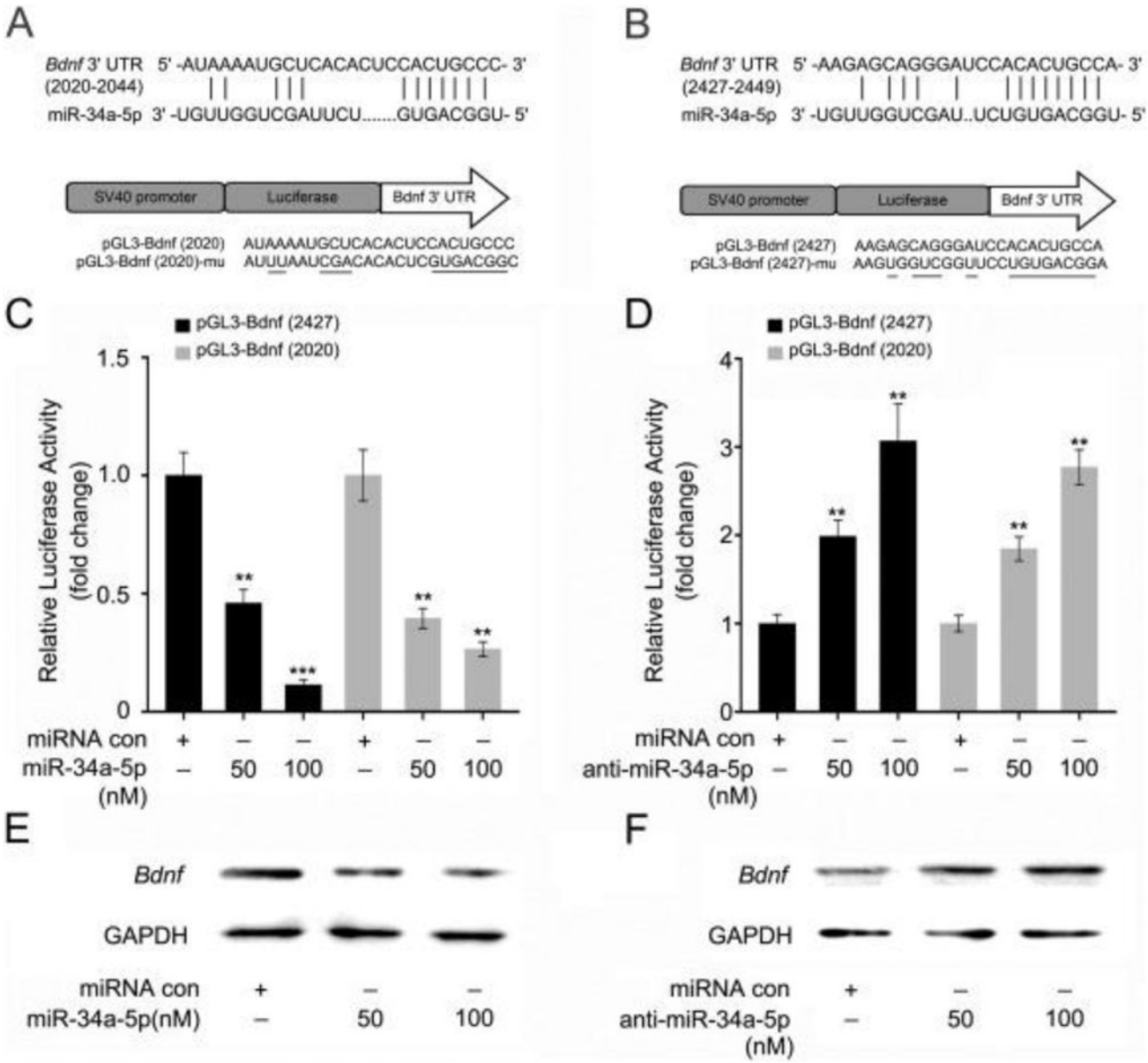

Figure 3. TAI-heightened miR-34a-5p down-regulates *Bdnf* through targeting its 3′UTR

(A, B) miR-34a-5p inhibits the expression of *Bdnf* by targeting the 3′UTR of predicted binding sites at nucleotides 2020–2044 and 2427–2449 of *Bdnf* 3′UTR. The generated mutant sites at the *Bdnf* 3′UTR seed region are indicated. The wild-type *Bdnf* 3′UTR (or mutant) was inserted into the downstream of luciferase reporter gene immediately in the pGL3-control vector. (C, D) The effect of miR-34a-5p (or anti-miR-34a-5p) on the pGL3-Bndf-2427 and pGL3-Bndf-2020 reporters in 3T3 cells were measured by luciferase reporter assays. (E, F) The effect of miR-34a-5p (or anti-miR-34a-5p) on the expression of *Bdnf* in 3T3 cells was measured by Western blotting. Each experiment was repeated at least three times. Statistically significant differences are indicated: $^{**}P < 0.01$; $^{***}P < 0.005$; Student *t*-test.

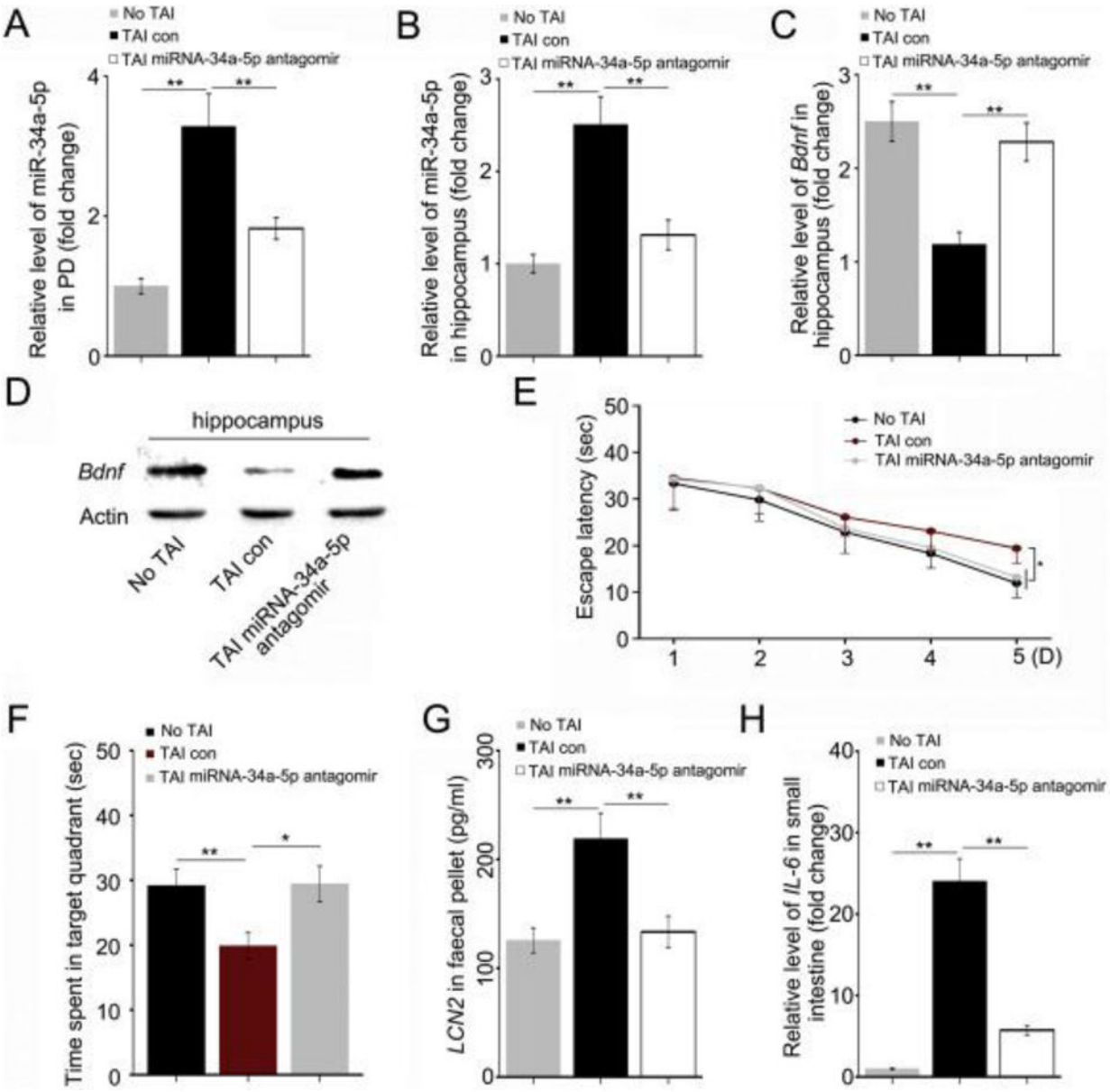

Figure 4. Tail intravenous injection of miR-34a-5p antagomir mitigates TAI-impaired cognitive function through restoring the expression of *Bdnf* in hippocampus

(A, B) The levels of miR-34a-5p in PB (A) and hippocampus (B) were assessed by qRT-PCR. The samples were obtained from mice without TAI, with TAI or treated with miR-34a-5p antagomir following TAI individually. $^{**}P < 0.01$; Student *t*-test, n = 12. (C, D) The mRNA and protein levels of *Bdnf* were assessed by qRT-PCR and Western blotting in hippocampus. The hippocampi were acquired from the above three cohorts. $^{**}P < 0.01$; Student *t*-test, n = 12. (E) The escape latency time to reach the hidden platform during the 5 days of Morris water maze test was assessed. $F_{(1, 47)} = 4.399$ between control and TAI group, $F_{(1, 47)} = 4.988$ between TAI and TAI with miR-34a-5p antagomir group, $^{*}P < 0.05$, ANOVA, n = 12. (F) The times spent in target quadrant and swimming traces in 60 s at day 6 of Morris water maze were shown. $F_{(1, 11)} = 9.720$ between control and TAI group, $^{**}P <$

0.01; $F_{(1, 11)} = 9.484$ between TAI and TAI with miR-34a-5p antagomir group, $^{*}P < 0.05$, ANOVA, n = 12. (G) The level of faecal *LCN2* was measured by ELISA. The faeces pellets were acquired from the above three cohorts. (H) The mRNA level of *IL-6* in small intestine tissues was examined by qRT-PCR. The small intestine tissues were acquired from the above three cohorts. $^{**}P < 0.01$; Student *t*-test, n = 12.

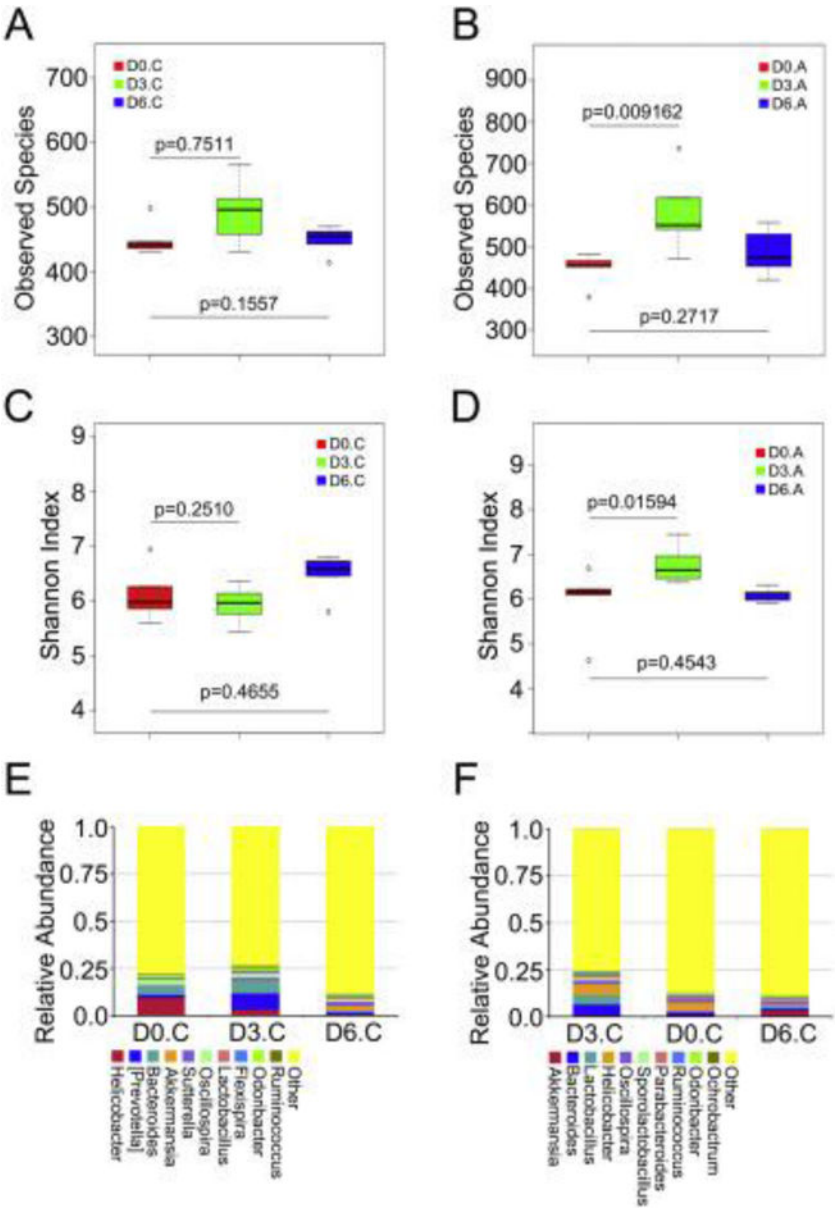

Figure 5. Tail Intravenous injection of miR-34a-5p antagomir shapes the frequency and community of gut microbiota after TAI

(A, B) The observed species number of intestinal bacteria in control (A) and miR-34a-5p antagomir treated (B) mice was examined by 16S high throughput sequencing after irradiation at days 3 and 6, n = 5 per group. Statistically significant differences are indicated: Wilcoxon rank sum test. (C, D) The Shannon diversity index of intestinal bacteria in control (C) and miR-34a-5p antagomir treated (D) mice was examined by 16S high throughput sequencing after irradiation at days 3 and 6, n = 5 per group. Statistically significant differences are indicated: Wilcoxon rank sum test. (E, F) The relative abundances of the top 10 bacteria at the genus level in control (E) and miR-34a-5p antagomir treated (F) mice were assessed using 16S high throughput sequencing after radiation at days 3 and 6, n = 5.

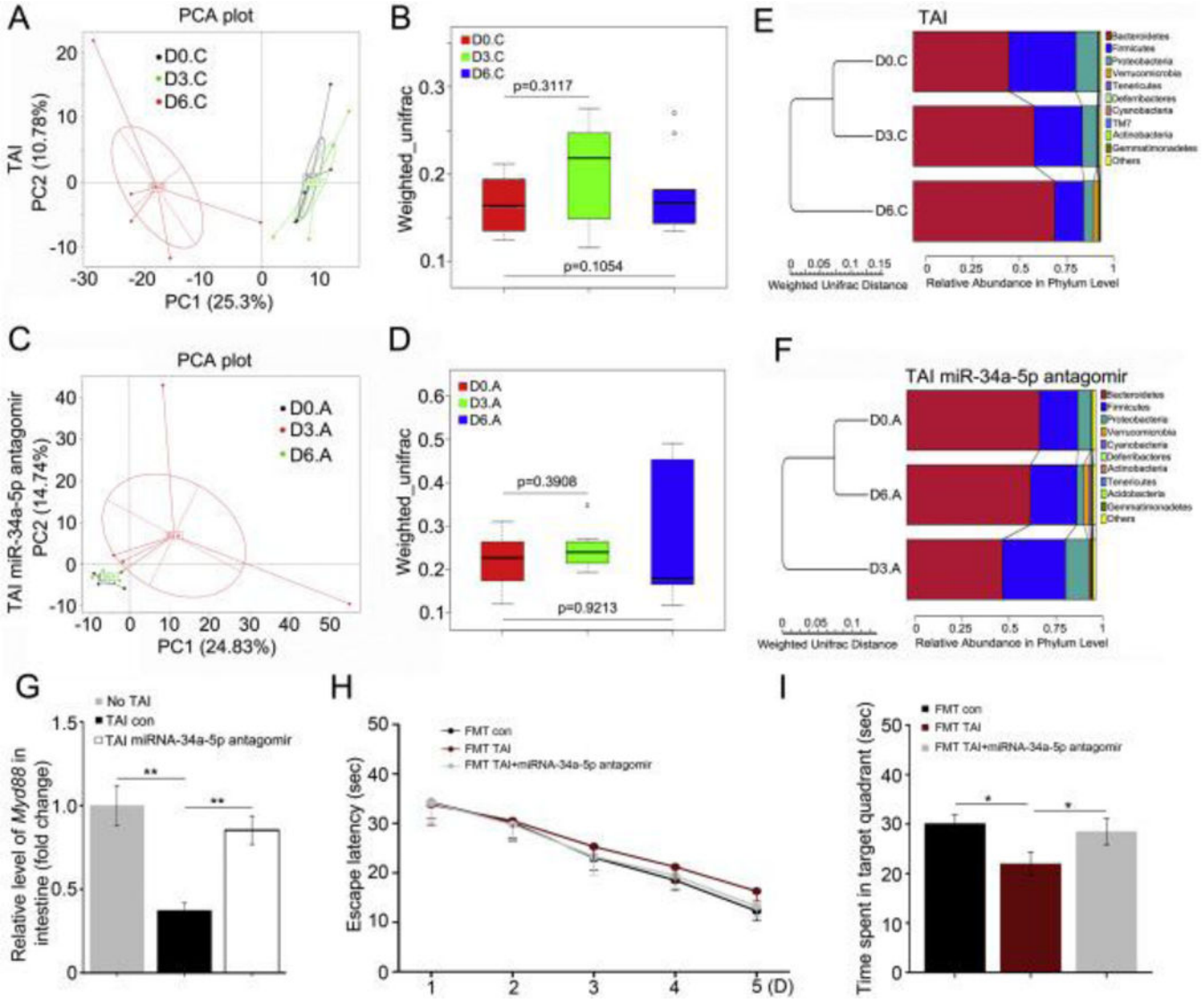

Figure 6. Administration of miR-34a-5p antagomir intravenous retains the intestinal bacterial community after TAI

(A, B) Principal component (A) and β diversity (B) analyses were used to measure the shift of intestinal bacterial flora profile in TAI exposure mice after radiation at day 3 and day 6, n = 5. Statistically significant differences are indicated: Wilcoxon rank sum test. (C, D) Principal component (C) and β diversity (D) analyses were used to measure the shift of intestinal bacterial flora profile in mice treated with miR-34a-5p antagomir following TAI at day 3 and day 6, n = 5. Statistically significant differences are indicated: Wilcoxon rank sum test. (E) The difference of intestinal bacterial structure at phylum level of mice on the day before TAI, day 3 and day 6 after TAI was examined using 16S high throughput sequencing, n = 5. (F) Tail intravenous injection of miR-34a-5p antagomir was performed immediately following TAI. The difference of intestinal bacterial structure at phylum level of mice on the day before TAI, day 3 and day 6 after TAI was examined using 16S high throughput sequencing, n = 5. (G) The mRNA level of *MyD88* in small intestine tissues was assessed by qRT-PCR. The samples were obtained from mice without TAI, with TAI or treated with

miR-34a-5p antagomir following TAI individually. $^{**}P < 0.01$; Student *t*-test, n = 12. (H) The escape latency time to reach the hidden platform during the 5 days of Morris water maze test was assessed. $F_{(1, 47)} = 3.443$ between control and FMT with TAI-exposed donors group, $F_{(1, 47)} = 0.993$ between FMT from TAI-exposed donors and FMT from TAI-exposed with miR-34a-5p antagomir injection group, $P > 0.05$, ANOVA, n = 12. (I) The times spent in target quadrant and swimming traces in 60 s at day 6 of Morris water maze were shown. $F_{(1, 11)} = 9.262$ between control and FMT with TAI-exposed donors group, $F_{(1, 11)} = 4.073$ between FMT from TAI-exposed donors and FMT from TAI-exposed donors with miR-34a-5p antagomir injection group, $^{*}P < 0.05$, ANOVA, n = 12.